BIROn - Birkbeck Institutional Research Online

Structure of the C-terminal Domain of the Prokaryotic Sodium Channel Orthologue NsvBa

W. C. Miller[a], A. J. Miles, B.A. Wallace[*]

Institute of Structural and Molecular Biology,

Birkbeck College,

University of London, London, UK

[a]Current Address: School of Biological Sciences, University of Kent, Canterbury, UK

*Author to whom correspondence should be addressed at:

Phone: 0207-631-6800

Fax: 0207-631-6803

Email: b.wallace@mail.cryst.bbk.ac.uk

Running Title: SRCD Analysis of the NsvBa C-terminus

Key words: Voltage-gated sodium channels, synchrotron radiation circular dichroism spectroscopy, structure prediction, bioinformatics, coiled-coil

Abstract

Crystallographic and electrophysiological studies have recently provided insight into the structure, function and drug binding of prokaryotic sodium channels. These channels exhibit significant sequence identities, especially in their transmembrane regions, with human voltage-gated sodium channels. However, rather than being single polypeptides with four homologous domains, they are tetramers of single domain polypeptides, with a C-terminal domain (CTD) composed of an inter-subunit four helix coiled-coil. The structures of the CTDs differ between orthologues. In NavBh and NavMs, the C-termini form a disordered region adjacent to the final transmembrane helix, followed by a coiled-coil region, as demonstrated by synchrotron radiation circular dichroism (SRCD) and double electron-electron resonance electron paramagnetic resonance spectroscopic measurements. In contrast, in the crystal structure of the NavAe orthologue, the entire C-terminus is comprised of a helical region followed by a coiled-coil. In this study we have examined the CTD of the NsvBa from *Bacillus alcalophilus,* which unlike other orthologues is predicted by different methods to have different types of structures: either a disordered adjacent to the transmembrane region, followed by a helical coiled-coil, or a fully helical CTD. To discriminate between the two possible structures we have used SRCD spectroscopy to experimentally determine the secondary structure of the C-terminus of this orthologue and used the results as the basis for modelling the transition between open and closed conformations of the channel.

Introduction

In eukaryotes voltage-gated sodium channels are responsible for the propagation of action potentials in excitable cells. Mutations in human Navs result in a wide range of neurological and cardiovascular diseases, making them important therapeutic targets. As such, there has been great interest in their structure. However the large size and complexity of eukaryotic Navs has made them impractical targets for structural studies. Much of our current knowledge of Nav structures comes from the simpler prokaryotic Nav orthologues which form homotetramers from four identical subunits (as opposed to pseudotetramers composed of four homologous domains of a single polypeptide in eukaryotic Navs). The crystal structures of a number of prokaryotic Navs determined in recent years (Payandeh et al. 2011; McCusker et al. 2012; Zhang et al. 2012; Shaya et al. 2014) have greatly expanded our understanding of their structure/function relationships (reviewed in (Catterall 2014)). However, with one exception (Shaya et al. 2014), the C-terminal domains (CTDs) (beyond the last transmembrane helix) of all of the orthologues studied were not visible in the crystal structures, despite their being physically present in the protein constructs studied. Synchrotron radiation circular dichroism (SRCD) and electron paramagnetic resonance-pulsed double electron resonance spectroscopic studies, and *in-silico* analysis of two of the functionally-active orthologues, NavBh (otherwise known as NaChBac, from *Bacillus halodurans*), and NavMs (from *Magnetococcus magnus*), indicated that their C-terminal domains consisted of a distal coiled-coil, connected to the intracellular C-terminal end of the final transmembrane segment (designated S6) by a flexible, disordered "neck" region (Powl et al. 2012; Bagnéris et al. 2013) (Figure 1 left). In the latter case, because there was also a crystal structure of the open state NavMs pore, it was possible to discern where the CTD structure proposed based on spectroscopy methods would fit within the disordered region in seen in the NavMs crystal (Powl et al. 2012). The presence of disordered regions between S6

and the C-terminal coiled-coil contrasted with the CTD visible in the closed form crystal structure of the NavAe orthologue from *Alkalilimnicola ehrlichei*, in which an almost completely helical neck region preceding the C-terminal coiled-coil could be seen (Shaya et al. 2014) (Figure 1 right). Interestingly, NavAe only exhibited measurable conductance in constructs in which the "neck" helical region was mutated, whereas both wildtype NavMs and NavBh supported conductance (Ren et al. 2001; Bagnéris et al. 2013).

In order to examine the structure of another prokaryotic Nav C-terminus which might be fully helical, we performed *in silico* structural analyses. The recently characterised Nav orthologue NsvBa (DeCaen et al. 2014) was identified by PsiPred secondary structure prediction as having a neck region likely to be helical. However DisoPred disorder prediction found the same region to be above the significance cut-off value for disorder prediction. This is unlike all other orthologues with structurally characterised C-termini, in all of which the PsiPred and DisoPred structural predictions agree with each other (and with the experimental data) as to the disordered/helical state of the neck region. Using a homology modelling approach, two NsvBa models were developed, one with a helical neck, the other with a disordered neck. Synchrotron Radiation Circular Dichroism spectroscopy of a series of C-terminal truncation constructs was then performed to characterise the secondary structural contents of the NsvBa C-terminus. This demonstrated that in NsvBa the neck region connecting the C-terminus to the pore is disordered, whilst the distal region of the C-terminus is helical, as in the NavMs and NavBh orthologues. These results may also support the model that the state of the C-terminus may influence the functional features and equilibria between channel conformational states, which furthermore may be inter-convertible and in equilibrium depending on their environment.

Materials and Methods

Materials

The NsvBa gene (DeCaen et al. 2014) was provided by Drs. Paul DeCaen and David Clapham (Harvard Medical School). A pore-only construct starting from residue 138 (with the addition of a preceding start codon) was cloned into the PET15B vector using NdeI/BamHI restriction sites. Truncation constructs were generated via site-directed mutagenesis, by mutating the listed residue number (265, 259, 250, 239, and 234) into a stop codon (Figure 2).

Protein ~~Expression and~~ Purification

Cell growth and membrane preparations were performed as previously described for NavBh (Powl et al. 2010), with the following modifications: Protein was eluted using a gradient of 80-500 mM imidazole, and purified samples were concentrated in a 50 kDa molecular weight cutoff concentrator (Pierce, Leicestershire, UK). Gel filtration chromatography was performed in 20 mM M sodium phosphate, pH 7.8, 0.02 % DDM, 50 mM NaCl, the conditions under which all of the SRCD measurements were conducted.   Protein yields were between 0.1 mg and 0.5 mg from 30 litres of culture. The predicted molecular masses of the NsvBa constructs are as follows: NsvBa 138-277: 16.1 kDa, NsvBa 138-265: 14.6 kDa, Nsvba 138-159: 13.8 kDa, NsvBa 138-250: 12.7 kDa, NsvBa 138-239: 11.5 kDa, NsvBa 138-234: 10.9 kDa. Full length protein identity was confirmed by fragmentation mass spectrometry of the 277 construct (done at the Protein and Nucleic Acid Chemistry Facility, Cambridge University, UK), in which peptides comprising both the N- and C-termini were detected. The Western blots seemed to indicate that the truncated constructs migrate at higher molecular masses than the full length construct, but it is the full-length construct that

migrates at a mass that is apparently too low (and hence why mass spectrometry was used to determine the presence of both termini). This aberrant running of full length constructs has also been observed for other orthologues (e.g. NaChBac, NavSp) (Nurani et al, 2008; McCusker et al, 2011).

Synchrotron Radiation Circular Dichroism (SRCD) Spectroscopy

The extinction coefficient of each protein construct was calculated from its amino acid sequence utilising Expasy ProtParam (Gasteiger E. 2005), and used to determine the concentration by triplicate measurements of the absorbance at 280 nm on a Nanodrop 1000 UV spectrophotometer (replicate values reproducible to within 1-5%).

SRCD spectra were collected on the DISCO beamline at the Soleil Synchrotron, France, and on beamline CD1 at the ISA synchrotron, Denmark, and at the CD12 beamline at the ANKA synchrotron, Germany, using protein concentrations in the range of 1 - 4mg/ml, in a Suprasil demountable cell (Hellma, Germany), pathlength 0.01 cm, over the wavelength range from 260 nm to 175 nm in triplicate, using a 1 nm step size and a dwell time of two seconds. Three baseline spectra, consisting of the corresponding flow-through from the concentration step, were averaged and subtracted from the averaged sample spectra. The resulting spectra were calibrated against a spectrum of camphoursulfonic acid collected after each synchrotron beam fill (Miles et al. 2003). Data processing was carried out using CDTools software (Lees et al. 2004). The spectra were truncated to 180 nm (the wavelength indicated by the HT cutoff criterion (Miles and Wallace, 2006), smoothed with a Savitsky-Golay filter, and scaled to delta epsilon values using mean residue weight values calculated for each construct (114.3, 113.9, 113.4, 12.7, 112.5, and 112.6 for full length, for 277, Δ265, Δ259, Δ250, Δ239, and Δ234, respectively, and analyses used the DichroWeb analysis server

(14) with the CONTINLL algorithm (Provencher and Glöckner 1981; Van Stokkum et al. 1990), and the MP180 reference set (Abdul-Gader et al. 2011).

C-terminal truncation analysis calculations used the helical percentage calculated for each construct. This value was then multiplied by the amino acid length of the construct, and subtracted from the value [helix x length] obtained for the pore with the full length C-terminus construct (residues 138-277), in each case taking into account the disordered hexahistidine tag. Values shown are the averages from three replicate sets of SRCD measurements.

Data Deposition

Spectral and metadata were deposited in the Protein Circular Dichroism Data Bank (Whitmore et al 2011) with codes CD0005306000 through CD0005333000.

Bioinformatic Analyses

Sequence alignments for NsvBa (accession WP_003324108), NavMs (UniProt ID A0L5S6), NavBh (UniProt ID D0RMU8), and NavAe (UniProt ID Q0ABW0) were performed using Clustal Omega (Sievers et al. 2011). Initial homology modelling was performed with the Phyre2 server using 1 to 1 threading (Kelley et al. 2015) and refined in Modeller (Eswar et al. 2006). Image generation and further model refinement was performed in Pymol (DeLano 2002). Sequence structure predictions were performed on the PsiPred server, using the PsiPred and DisoPred functions (McGuffin et al. 2000; Ward et al. 2004). The COILS server v2.2 (Lupas et al. 1991) was used for prediction of the coiled-coil, and identification of the heptad repeat positions.

Results

Bioinformatics and Modelling of the CTD

The full length NsvBa, NavBh, NavMs, and NavAe sequences were analysed using the PsiPred algorithm, which correctly identified the expected six transmembrane helices identified in previous structural studies (Payandeh et al. 2011; McCusker et al. 2012; Zhang et al. 2012; Shaya et al. 2014) for all sequences analysed (data not shown). For NavMs, NavBh, and NavAe, both PsiPred and DisoPred predictions (Figure 3) correlated with each other and with the experimentally-determined secondary structures of their C-termini. For NsvBa, PsiPred analysis predicted that the C-terminus would consist entirely of a single long helical region, continuing from the end of the S6 helix until near the end of the C-terminus, similar both to what was observed in the NavAe pore structure, and to the PsiPred prediction of the NavAe sequence (Figure 3). In contrast, the DisoPred disorder analysis of the NsvBa sequence for the neck region (residues 236 to 249) was above the significance cutoff value for intrinsic disorder prediction, similar to what was been observed in predictions and structural studies of NavMs and NavBh (Figure 3).

Based on these conflicting predictions, two models of NsvBa were developed: A model with a disordered neck region (Figure 4 left) was generated using the NavMs pore structure (Bagnéris et al. 2013) and a model with a helical neck region (Figure 4 right) was generated using the NavAe pore structure (Shaya et al. 2014). It should be noted that the in the NavMs crystal structure, the pore was in an open conformation, whereas the NavAe crystal structure had a closed pore. These pore states were retained in the corresponding NsvBa models.

The sequence alignments indicate that while the transmembrane helices are well conserved, there is lower similarity between the C-termini of the orthologues, although a region with a stretch of charged residues within the neck region is conserved. All four sequences display the heptad repeat characteristic of a coiled-coil at the end of the CTD (Powl et al. 2012). This region has previously shown to be important for expression of the

channel, and has been proposed to have a role in channel assembly (Mio et al. 2010) and function (Powl et al. 2012).

SRCD Spectroscopy of the NsvBa pore and its C-Terminal Truncations

In order to determine which of the models better corresponds with the secondary structure of the NsvBa neck region, SRCD spectroscopic analysis of a series of C-terminal truncations of the NsvBa-pore was performed (Figure 5a). SRCD spectroscopy was utilised to determine small differences (high signal-to-noise) in the spectra that produce different secondary structure percentages between truncations, as the required discrimination between small spectral signals could not be achieved with a benchtop CD, especially for proteins which require high salt concentrations for stability (and hence necessitate the use of short pathlength cells.

An N-termainal truncation was used to produce pore-only constructs starting at the 138th residue, prior to the S5 helix (this corresponds with the N-terminal ends of the NavMs and NavAe pore constructs) (McCusker et al. 2012; Shaya et al. 2014). Pore-only constructs (by comparison with full-length channels that also include the voltage-sensor domains) were previously shown to be active (McCusker et al. 2012; Shaya et al. 2014) and have virtually identical structures to the pore domains in intact prokaryotic sodium channels (Payandeh et al. 2011). In this study they were utilised in order to increase the percentage change seen in secondary structure resulting from serial truncations of the C-terminus. C-terminal truncations designated Δ265, Δ259, and Δ250 (in which the indicated residue has been mutated to a stop codon) expressed well, but exhibited apparent increased molecular mass in SDS-PAGE gels (Figure 2b) in constructs both with the voltage sensor, and pore-only constructs. The observation that the locations of SDS-PAGE bands do not correlate precisely with molecule mass is not unusual for membrane proteins in general (Rath et al. 2009) and

also specifically for sodium channels (Powl et al. 2010; McCusker et al. 2012); mass spectrometry confirmed their identity as NsvBa (data not shown).

In both the disordered and helical neck models, the coiled-coil helix was predicted to extend from residue 250 to just prior to the end of the sequence. In all three truncations, the calculated number of helical residues removed correlated well with the predicted helical residues removed (Table 1), indicating that this entire region is helical, and likely forms the predicted coiled-coil. For the Δ239 and Δ234 constructs, the helical neck model predicts the removal of 39 and 40 helical residues, respectively. In each of them a large helical segment, stretching from 250-238, as well as a small disordered segment, 237-234, would be removed. In the disordered neck model, the same region is almost entirely disordered, and the model predicts that only 27 and 28 residues are helical of the total 43 and 38 residues removed by truncation at these positions (Figure 5b). Calculations of the helical contents were within one standard deviation of the calculated changes in the percentages of helix in the disordered neck model of the NsvBa C-terminus, for both the Δ239 and Δ234 constructs (Table 1), but differed significantly from calculated changes for the helical neck. This provided strong evidence that the NsvBa the neck region is disordered, consisting of approximately 16 residues, as in the Figure 4 disordered neck model.

The possibility that NsvBa could transition between the two models was also considered. If the presence of the coiled-coil stabilised the neck region in a helical conformation, then complete removal of the coiled-coil in Δ250 could have resulted in the neck region shifting from a helical to a disordered conformation. This would have been observed as the loss of 40 helical residues in Δ250 as compared to the full length C-terminus; however this was not observed. It was also possible that the C-termini exist as a mixed population of helical and disordered neck regions within the sample. This would have been observable as the calculated number of residues removed being somewhere between the

10

predictions for the two models, as the residues removed could be considered to be partially helical. As the calculated number of helical residues removed were within one standard deviation of the predictions based upon the disordered neck model, this offers no support for either helical-disorder transition hypothesis under the conditions used in the present study, where the open/closed state of the pore is unknown. The results may suggest that like NavMs, the NsvBa channel is in the open conformation. It is possible that the neck could undergo a structural change associated with the conformational state of the channel. However this is not yet testable since to date no means has yet been found to produce a specific conformational state for any of the sodium channels, and the secondary structures (but not tertiary structures) of the open and closed states are the same despite a rotation about one residue in the S6 helix that alters the opening of the intracellular side of the pore (Powl et al. 2012).

<u>Discussion</u>

The SRCD spectroscopic analyses in this study have indicated that the neck region of the CTD of the NsvBa channel consists of approximately 16 disordered residues, with the remaining 27 residues in a helical structure, mostly likely a coiled-coil. The distal coiled-coil is predicted for all known prokayotic Nav orthologues (Figure 4) and may have a role in stabilising the tetrameric channels, but such a structure is not found (or necessary) in eukaryotic Navs, which are formed of single polypeptide chains; this is a major difference between human and bacterial channels. Unlike eukaryotic C-termini which are proposed to form a "ball and chain" like structure that plays a role in fast inactivation, prokaryotic Navs have only been observed to undergo slow inactivation processes.

It has been shown that the coiled-coil structure is not essential for membrane insertion or tetramer assembly, but may be involved in stabilising the tetrameric structure (Mio et al. 2010; Powl et al. 2010; Bagnéris et al. 2013). It has been proposed that the flexible neck

region could play a role in regulating in the opening and closing of the pore (Bagnéris et al. 2013), by enabling the splaying of the C-terminal ends of the S6 helices without interrupting the hydrogen bonds present in an ordered structure. This would enable a faster and energetically less costly channel conformation change during gating. During channel gating, the neck could act like a spring or tether separating the stabilising coiled-coil from the moving S6 helixes. While the conflicting predictions for disorder and helical structure within the neck region of NsvBa support this hypothesis, such predictions were not observed in any other structurally characterised channel. Additionally, no evidence for a helix-to-disorder transition of this region in NsvBa was observed under the conditions of this study, even upon truncation of the coiled-coil, nor did the results suggest a mixed population of helical and disordered conformations of the neck region within the sample. However, under the conditions used (detergent micelles) there is no driving force such as an ion gradient, to initiate such a transition between conformational states, which would be the likely instigator for any change in the secondary structure within the CTD neck region. This lack of driving force for conformational change is also true for the other crystallographic or spectroscopic studies of the prokaryotic channels, as all of them also utilised detergent micelles or bicelles to maintain channel solubility. Detailed studies involving subtle changes such as the ones described in this work would not have been feasible in lipid bilayers due to scattering/absorption flatting artefacts present in membrane samples (Wallace 2009). The results obtained in this study are consistent with the NsvBa pore being in the open conformation (such as NavMs, which also has a disordered neck region), although it is possible that opening/closing of the pore could modify the conformation of the neck to that seen in the closed state structure of NavAe (the wild type of which, curiously, shows no conductance, suggesting that the closed conformation is highly stable under the experimental

conditions used in that study). Assessment of this, however, will await production of corresponding open and closed crystal structures for those orthologues.

References

Abdul-Gader A, Miles AJ, Wallace BA (2011) A reference dataset for the analyses of membrane protein secondary structures and transmembrane residues using circular dichroism spectroscopy. Bioinformatics 27:1630–1636

Bagnéris C, DeCaen PG, Hall BA, Naylor CE, Clapham DE, Kay CWM, Wallace BA (2013) Role of the C-terminal domain in the structure and function of tetrameric sodium channels. Nat Comm 4:2465

Catterall WA (2014) Structure and function of voltage-gated sodium channels at atomic resolution. Experimental Physiology 99:35–51

DeCaen PG, Takahashi Y, Krulwich TA, Ito M, Clapham DE (2014) Ionic selectivity and thermal adaptations within the voltage-gated sodium channel family of alkaliphilic Bacillus. Elife 3:04387

DeLano WL (2002) The PyMOL molecular graphics system.

Eswar N, Webb B, Marti-Renom MA, Madhusudhan M, Eramian D, Shen M, Pieper U, Sali A (2006) Comparative protein structure modeling using Modeller. Current Protocols in Bioinformatics. Chapter 5:6

Gasteiger E. BA Hoogland C. Gattiker A. Duvaud S. Wilkins M.R. Appel R.D. (2005) Protein identification and analysis tools in the ExPASy server. In: Link A. (eds) 2-D Proteome Analysis Protocols. Humana Press, pp 531–552

Kelley LA, Mezulis S, Yates CM, Wass MN, Sternberg MJE (2015) The Phyre2 web portal for protein modeling, prediction and analysis. Nat Protocols 10:845–858

Lees JG, Smith BR, Wien F, Miles AJ, Wallace BA (2004) CDtool-an integrated software package for circular dichroism spectroscopic data processing, analysis, and archiving. Anal Biochem 332:285–289

Lupas A, Van Dyke M, Stock J, et al. (1991) Predicting coiled coils from protein sequences. Science 252:1162–1164

McCusker EC, D'Avanzo N, Nichols CG, Wallace BA (2011) Simplified Bacterial "pore" provides insight into the assembly, stability and structure of sodium channels. J. Biol. Chem. 286:16386-16391.

McCusker EC, Bagnéris C, Naylor CE, Cole AR, D'Avanzo N, Nichols CG, Wallace BA (2012) Structure of a bacterial voltage-gated sodium channel pore reveals mechanisms of opening and closing. Nat Comm 3:1102

McGuffin LJ, Bryson K, Jones DT (2000) The PSIPRED protein structure prediction server. Bioinformatics 16:404–405

Miles AJ, Wallace BA (2006) Synchrotron radiation circular dichroism spectroscopy of proteins and applications in structural and functional genomics. Chem. Soc. Reviews 35:39-51.

Miles AJ, Wien F, Lees JG, Rodger A, Janes RW, Wallace BA (2003) Calibration and standardisation of synchrotron radiation circular dichroism and conventional circular dichroism spectrophotometers. Spectroscopy 17:653–661

Mio K, Mio M, Arisaka F, Sato M, Sato C (2010) The C-terminal coiled-coil of the bacterial voltage-gated sodium channel NaChBac is not essential for tetramer formation, but stabilizes subunit-to-subunit interactions. Progress in Biophysics and Molecular Biology 103:111–121

Nurani G., Radford M., Charalambous K., O'Reilly AO, Cronin N, Haque S, Wallace BA (2008) Tetrameric bacterial sodium channels: characterisation of structure, stability, and drug binding. Biochemistry 47:8114-8121.

Payandeh J, Scheuer T, Zheng N, Catterall WA (2011) The crystal structure of a voltage-gated sodium channel. Nature 475:353–358

Powl AM, Miles AJ, Wallace BA (2012) Transmembrane and extramembrane contributions to membrane protein thermal stability: Studies with the NaChBac sodium channel. Biochim Biophys Acta - Biomembranes 1818:889–895

Powl AM, O'Reilly AO, Miles AJ, Wallace BA (2010) Synchrotron radiation circular dichroism spectroscopy-defined structure of the C-terminal domain of NaChBac and its role in channel assembly. Proc Natl Acad Sci (USA) 107:14064–14069

Provencher SW, Glöckner J (1981) Estimation of globular protein secondary structure from circular dichroism. Biochemistry 20:33–37

Rath A, Glibowicka M, Nadeau VG, Chen G, Deber CM (2009) Detergent binding explains anom*alous SDS-PAGE migration of membrane proteins. Proc Natl Acad Sci (USA) 106:1760–1765

Ren D, Navarro B, Xu H, Yue L, Shi Q, Clapham DE (2001) A prokaryotic voltage-gated sodium channel. Science 294:2372–2375

Shaya D, Findeisen F, Abderemane-Ali F, Arrigoni C, Wong S, Nurva SR, Loussouarn G, Minor DL (2014) Structure of a prokaryotic sodium channel pore reveals essential gating elements and an outer ion binding site common to eukaryotic channels. J Mol Biol 426:467–483

Sievers F, Wilm A, Dineen D, Gibson TJ, Karplus K, Li W, Lopez R, McWilliam H, Remmert M, Söding J, others (2011) Fast, scalable generation of high-quality protein multiple sequence alignments using Clustal Omega. Mol Systems Biol 7:539

Van Stokkum IH, Spoelder HJ, Bloemendal M, Van Grondelle R, Groen FC (1990) Estimation of protein secondary structure and error analysis from circular dichroism spectra. Anal Biochem 191:110–118

Wallace BA (2009) Protein characterisation by synchrotron radiation circular dichroism spectroscopy. Quart Rev Biophys 42:317–370

Ward JJ, McGuffin LJ, Bryson K, Buxton BF, Jones DT (2004) The DISOPRED server for the prediction of protein disorder. Bioinformatics 20:2138–2139

Whitmore, L., Woollett, B., Miles, A.J., Klose, D.P., Janes, R.W., and Wallace, B.A.(2011) PCDDB: The protein circular dichroism data bank, a repository for circular dichroism spectral and metadata. Nucl Acids Res 39:D480-D486.

Zhang X, Ren W, DeCaen P, Yan C, Tao X, Tang L, Wang J, Hasegawa K, Kumasaka T, He J, et al (2012) Crystal structure of an orthologue of the NaChBac voltage-gated sodium channel. Nature 486:130–134

Figures:

Figure 1. Structures of Nav C-Termini. A) Schematic diagram of models of Nav pores in different states. The open form has a disordered neck with a helical coiled-coil C-terminus, while the closed form has a helical neck with a coiled-coil C-terminus. Only two monomers of each tetramer are shown for clarity. The S5 helices are in pink, the S6 helices in blue, the neck regions in cyan, and the coiled-coils are in orange. B) Corresponding structures of NavMs (crystal/DEER spectroscopy) (Powl et al. 2012)/NavBh (SRCD spectroscopy) (6), and NavAe (crystal) (4), in which the four monomers in each tetramer are depicted in different colours.
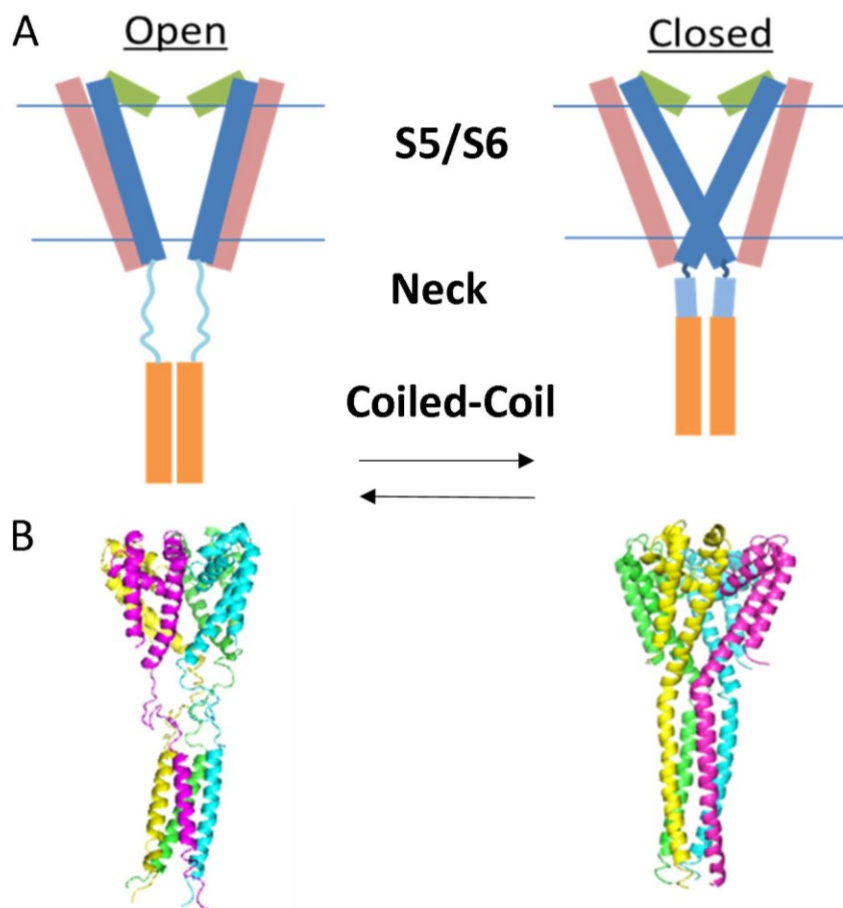
Figure 2. The NsvBa C-Terminal Truncation Constructs. A) Sequences (and nomenclatures) of the NsvBa pore C-terminal truncations created: 277 denotes a (wild type) pore-only construct (in which the voltage sensor has been removed) with a full length C-terminus; the other constructs are numbered based on the residue at which the construct has been truncated by mutation to a stop codon. The locations of the ends of the S6 helix and the coiled-coil regions are indicated above the sequences. B) Western blot analysis of the NsvBa pore and truncated constructs.

A

	S6	Coiled-coil
277	FIGVIVNNVEKANEDEVKDKVKEKEEAAQKQMDSLHEELKEIKQYLKSIEKQNRSS
Δ265	FIGVIVNNVEKANEDEVKDKVKEKEEAAQKQMDSLHEELKEIK
Δ259	FIGVIVNNVEKANEDEVKDKVKEKEEAAQKQMDSLHE
Δ250	FIGVIVNNVEKANEDEVKDKVKEKEEAA
Δ239	FIGVIVNNVEKANEDEV
Δ234	FIGVIVNNVEKA

B

277 Δ265 Δ259 Δ250 Δ239 Δ234

50 kDa

20 kDa

Figure 3. Predictions for Secondary Structure of the C-Termini. The sequences for four

orthologues of bacterial sodium channels (NsvBa, NavAe, NavMs, and NavBh) are shown.

Predictions were performed on the full length amino acid sequences, however for simplicity,

in this figure the sequences are shown starting from the middle of the S6 helix (the end of S6

is indicated by the dotted vertical line) to the end of the C-termini, starting at the numbered

residue listed under the name. The hydrophobic positions of the heptad repeat (positions a

and d) are highlighted in grey for predicted coiled-coil regions. A vertical dotted line marks

the end of the S6 transmembrane helix. In the Psipred prediction, residues marked H denote

helical predictions, residues marked C denote disordered predictions, with the cylinders

above each sequence corresponding to where the predicted helical regions are. In the

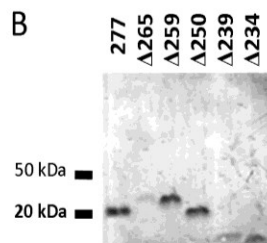Disopred prediction, residues predicted to be disordered are indicated with a *.

Figure 4. Homology Models of Different Potential Conformations of the NsvBa C-terminus. Disordered neck model based on NavMs (left), and the helical neck model based on NavAe (right). Monomers of each are shown. The approximate positions of the truncation constructs are indicated with labelled arrows. "277" corresponds to the full length protein. The images were generated in Pymol (21).
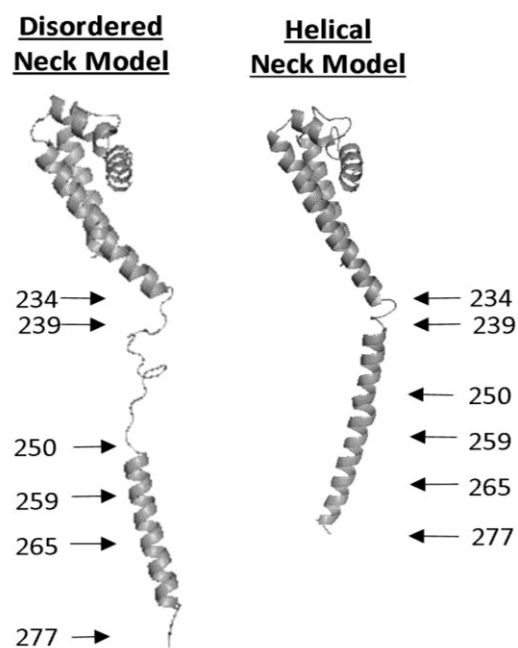
Figure 5. SRCD Spectroscopy of NsvBa Truncations. A) SRCD spectra of several representative constructs of NsvBa pore: FL (solid line), D250 (dotted line), and D234 (dashed line). Error bars are one standard deviation of the three repeat measurements. B) Plot of number of helical residues removed versus construct length, based on SRCD data (solid line), and predicted helical residues removed for Disordered Neck (dashed line, triangle marker), Helical Neck (dotted line, square marker), and Transition models (dashed/dotted line, circle marker).

A
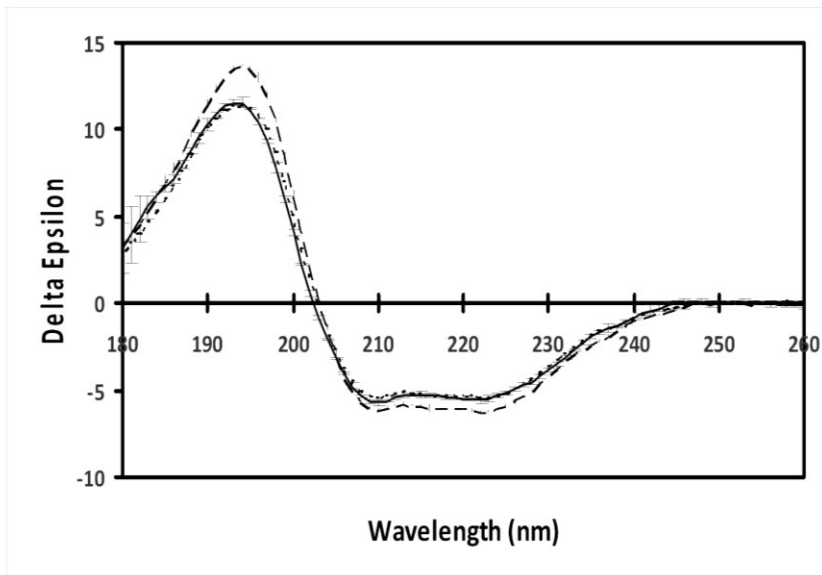
B
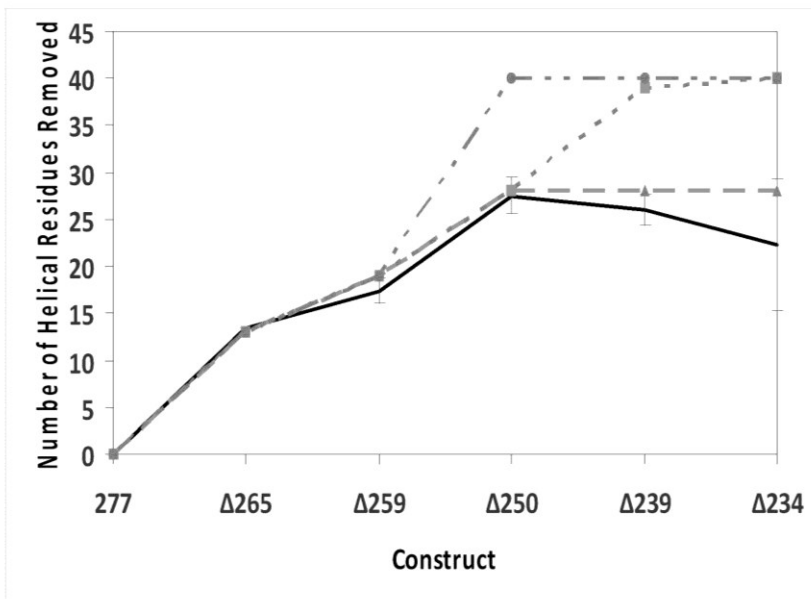
Tables:

Table 1. Calculated Effects of Removing Residues. Calculated number of helical residues removed (based on the experimental SRCD data) compared with predicted numbers of helical residues removed for the Disordered Neck, Helical Neck, and Transition models. Predictions were obtained by determining the number of residues in the secondary structure of each removed section of the corresponding model. +/- values are from calculations on three repeat sets of measurements (consisting of 3 scans each) of the experimental data.

Construct	Calculated Number of Helical Residues Removed: Experimental Data	Predicted Number of Helical Residues Removed (Disordered Neck Model)	Predicted Number of Helical Residues Removed (Helical Neck Model)	Predicted Number of Helical Residues Removed Transition Model)
277 (WT)	0	0	0	0
Δ265	13.5 +/- 0.0	13	13	13
Δ259	17.4+/- 1.4	19	19	19
Δ250	27.5+/- 2.0	28	28	40
Δ239	26.0 +/- 1.6	28	39	40
Δ234	22.3 +/- 7.0	28	40	40